PRELIMINARY STUDY ON SST FORECAST SKILL ASSOCIATED WITH THE 1982/83 EL NIÑO PROCESS, USING COUPLED MODEL DATA ASSIMILATION

K. Miyakoda, J. Ploshay and A. Rosati

Reprinted from

ATMOSPHERE-OCEAN SPECIAL
Vol. XXXV, No. 1, pp. 469–486
March, 1997

PRINTED IN CANADA

Preliminary Study on SST Forecast Skill Associated with the 1982/83 El Niño Process, Using Coupled Model Data Assimilation

K. Miyakoda, J. Ploshay and A. Rosati
GFDL/NOAA Princeton University,
Princeton, NJ 08542, U.S.A.

[Original manuscript received 1 May 1995; in revised form 22 August 1995]

ABSTRACT *A previous study by Rosati et al. (1997) has concluded that the specification of an adequate thermocline structure along the equatorial Pacific ocean is most crucial for El Niño forecasts. In that paper, the oceanic initial condition was generated by a data assimilation (DA) system (Derber and Rosati, 1989). However, the initial condition for the atmospheric part was taken from the National Meteorological Center's (NMC) operational analysis, which was simply attached to the oceanic part for the coupled model forecasts.*

In the present paper, both the atmospheric and oceanic initial conditions are generated by a coupled DA system applied to a coupled air-sea general circulation model (GCM). The assimilation for the ocean is performed by the same system as mentioned above, in which the SST (sea surface temperature) and the subsurface temperatures are injected into a 15 vertical level oceanic GCM. The upper boundary condition, such as surface wind stress, is specified by the atmospheric DA. The assimilation for the atmosphere is performed by the continuous injection method of Stern and Ploshay (1992), using an 18 vertical level atmospheric GCM. The lower boundary condition, such as SST, is specified by the oceanic DA. The coupled model assimilations are carried out by switching the DA processes alternately every 6 hours between the ocean and the atmosphere.

The emphases of this study are: firstly, the effect of coupled air-sea model DA on the performance of subsequent forecasts; secondly, the impact of the coupled assimilation on improvement of the "spin-up" behaviour of forecasts, i.e. to see whether a smooth start to the forecast is achieved by the coupled model DA process; and thirdly, investigation of the effect that the "spring barrier" has on predictability in the coupled GCM system. Preliminary results indicate that, in order to answer these questions, ensemble forecasts are necessary. Besides, the coupled assimilation could be important in improving the overall behaviour of El Niño and La Niña forecasts.

RÉSUMÉ *Une étude antérieure de Rosati et al. (1955) a opiné que la prévision du El Niño dépend grandement de la spécification d'une structure thermocline adéquate sur l'océan Pacifique équatorial. Dans cette étude, la condition initiale océanique utilisait le système d'assimilation des données (DA) de Derber et Rosati (1989). Toutefois, la condition initiale de la partie atmosphérique était constituée de l'analyse régulière du NMC (National Meteorological center) qui était simplement rattachée à la partie océanique pour les prévisions du modèle couplé.*

Ici les conditions initiales, tant atmosphériques qu'océaniques, sont générées par un système DA couplé appliqué à un modèle de circulation générale (GCM) couplé air-mer. L'assimilation pour l'océan est effectuée par le même système que ci-dessus, dans lequel la température superficielle de la mer (SST) et les températures sous la surface sont injectées dans un GCM océanique à 15 niveaux verticaux. La condition à la couche limite supérieure, p. ex. la force d'entraînement du vent de surface, est déterminée par le système DA atmosphérique. L'assimilation pour l'atmosphère est accomplie par la méthode d'injection continue de Stern et Ploshay (1992), utilisant un GCM atmosphérique de 18 niveaux verticaux. Les conditions à la limite inférieure, telle que la SST, sont déterminées par le système DA océanique. Les assimilations du modèle couplé sont effectuées en enclenchant alternativement les processus d'assimilation de l'océan et de l'atmosphère à toutes les six heures.

L'étude porte surtout sur : l'effet du modèle avec système DA couplé air-mer sur la performance des prévisions subséquentes; l'impact de l'assimilation couplée sur l'amélioration du comportement de départ des prévisions (p. ex., un départ doux de la prévision résulte-t'il du système DA du modèle couplé) ; l'investigation de l'effet que la «barrière printannière» a sur la prévision dans le système de GCM couplé. Les premiers résultats indiquent que des prévisions d'ensembles sont nécessaires afin de répondre à ces questions. En outre, l'assimilation couplée pourrait être importante pour améliorer le comportement général de la prévision du El Niño et de LA Niña.

1 Introduction

Tropical oceanic-atmospheric forecasts have been considerably improved, using simple dynamical models or statistical methods (see Barnett et al., 1988). In this paper, however, the approach will be exclusively based on the coupled atmosphere-ocean general circulation models (GCMs). The issue is the seasonal forecasts, which treat the global oceanic and atmospheric states on the time ranges of about one year.

Concerning the activities related to the low frequency variation of the atmosphere, it is known (see for example, Brankovic et al., 1994) that the El Niño/Southern Oscillation signal is most dominant. This suggests that the forecast of ENSO should be of greatest concern in order to unravel the possibility of seasonal forecasting, and thereafter, further search for predictable elements should be pursued over other areas of the globe.

The simple model approach for El Niño prediction, such as Cane and Zebiak (1985) and Cane et al. (1986), treats the anomaly components of variables. On the other hand, the GCM approach has to treat the total components. This aspect presents one of the difficult and yet challenging problems in forecasts. An example is obtaining a good seasonal cycle of SST in the eastern equatorial Pacific, i.e., NINO-3 (150°W–90°W, 5°N–5°S) region, which is a formidable task. According to GCM experience (see for example, Neelin et al., 1992; Miyakoda et al., 1993), the coupling process is extraordinarily sensitive to the character of the atmospheric part of the physics and orographic or coast-line specifications.

Rosati et al. (1997) have shown successful forecasts, using a coupled oceanic-atmospheric GCM. The results are very encouraging. However, there are several issues that have to be made clear. They are: the limit of predictability, the spring barrier and the reduction of forecast errors associated with the initial spin-up problem. In order to investigate these issues, ensemble forecasts are useful or even required. If so, an adequate scheme for constructing the initial condition is essential. The main objective of this paper is to describe a DA system with a coupled oceanic-atmospheric GCM.

2 Background

Rosati et al. (1996) reported the results of 13-month forecasts, using a coupled atmospheric-oceanic GCM with fine equatorial resolution.

a *Model*

The atmospheric part has spectral triangular truncation at zonal wavenumber 30, corresponding to 4.0° longitude × 4.0° latitude (see Laprise, 1993) and 18 vertical levels. On the other hand, the oceanic part has a 1° × 1° longitudinal and meridional resolution outside of 10°N–10°S and 1/3° inside of the equatorial zone (Philander and Seigel, 1985). A set of adequate subgrid-scale physics for the atmosphere and ocean model is included. The prediction domain is the entire global atmosphere and the world ocean between 65°N and the Antarctic. All forecasts in this paper *do not* include flux corrections (Sausen et al., 1988).

The atmosphere and ocean models are coupled by exchanging the fluxes of momentum, heat, radiation and the SST specification with each other.

b *Initial conditions*

The inclusion of adequate information in the initial conditions is of considerable importance for weather forecasts; it may also be true for seasonal forecasts.

As the first step toward coupled model prediction, a scheme of oceanographic DA was developed by Derber and Rosati (1989). This was based on the variational method, in which various constraints are included to specify dynamical formulae and observational accuracies. Through these constraints, the observed SST and subsurface data, XBT (expendable bathythermograph) and others, are injected into the ocean model through the optimum interpolation scheme (OI). The upper boundary conditions of the ocean GCM are specified by surface wind stress, atmospheric heat flux, moisture flux and incoming shortwave and net longwave radiation. Most of these data are taken from the NMC (National Meteorological Center) operational analysis, with the exception that the radiation is given by the seasonally varying climatologies. The ocean model is integrated forward in time for many years (1979–1988), while these data are continuously injected and assimilated into the model (see Rosati et al., 1995 for more detail).

c *Cases*

The forecast cases consist of 7 episodes starting from January or July every year for the 7 years of 1982–1988. During this 7-year period, there are two distinct El

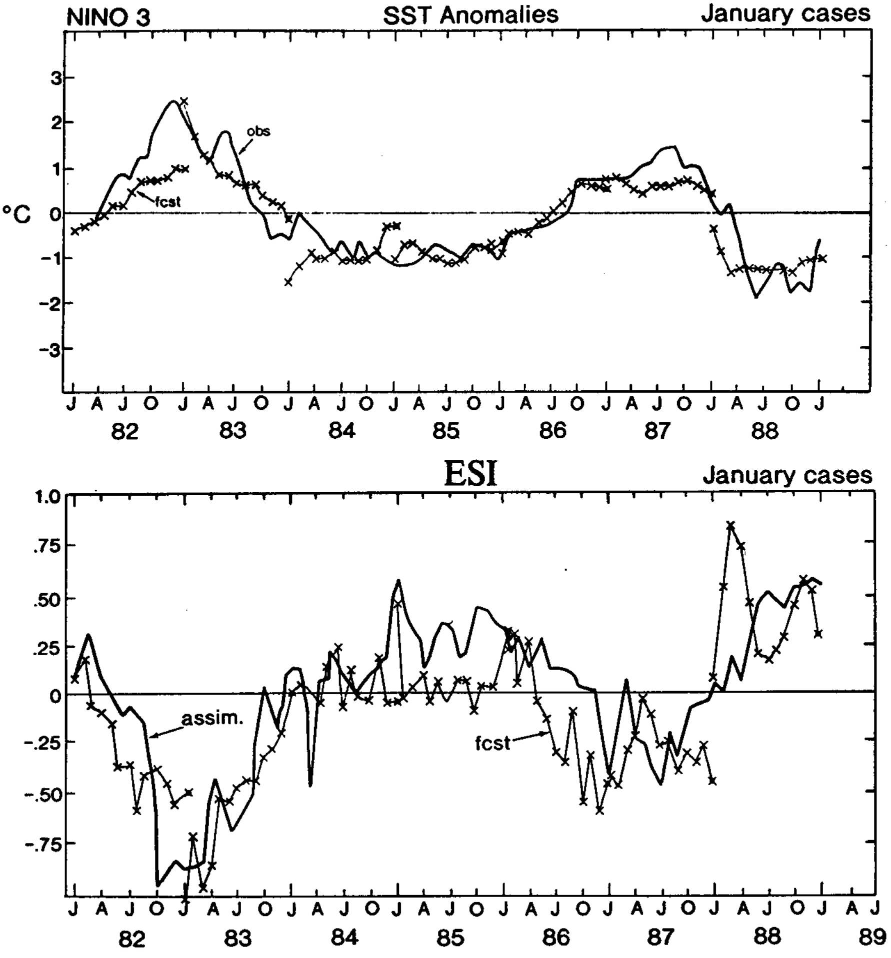

Fig. 1 Performance of the 13-month forecasts is shown by SST anomalies for NINO-3 region (upper) and ENSO indices, i.e. *ESI* (lower). Thick curves are the observations, and the curves connected with crosses are the forecasts (after Rosati et al., 1997).

Niño events and two events of La Niña. The initial condition time is 0000 GMT on the first day of January or July. The time range of the forecasts is 13 months.

d *Prediction skill*

The results of the 7 January forecasts are displayed in Fig. 1. For each month of the forecasts, the monthly mean SST anomaly was computed over the NINO-3 region and is shown in the upper panels. The lower panel is the zonal mean heat content anomaly index or ENSO index, i.e. ESI, which will be explained below.

For the atmosphere alone, the SOI (Southern Oscillation Index) is a traditional indicator of the low-frequency atmospheric oscillation, which operates over the semi-global domain (Troup, 1965; Trenberth, 1976). On the other hand, for the coupled system, other indices appear to be more appropriate. The first measure is of the west-east tilt of the 20° isotherm along the equatorial Pacific, which is defined by

$$GRD = (D_w - D_e)/110 - 1 \tag{1}$$

where D is the depth of the 20° isotherm, and D_w and D_e are its depths at 160°E and 90°W respectively. The mean value of $D_w - D_e$ is 110 metres, i.e. $160 - 50 = 110$. When *GRD* is negative, the situation corresponds to the warm phase in the eastern tropical Pacific, i.e. El Niño, while when the *GRD* is positive, the situation corresponds to the cold phase, i.e. La Niña.

In order to eliminate the seasonality of the DA, the anomaly of *GRD* is calculated, in a similar way as for the SOI. This anomaly is referred to as the ENSO index, or simply *ESI*, i.e.

$$ESI = GRD - \overline{GRD} \tag{2}$$

where $\overline{GRD}$ is the average over multiple years for the respective month, and it is, therefore, a function of Julian day (or month).

The continuous thick line curves in Fig. 1 are observed SST anomalies for the NINO-3 region (upper panel), after Reynolds (1988), and the *ESI* from the DA (lower panel). The thin line curves with crosses are the SST and *ESI* anomalies from the 7 forecast cases, each run for 13 months. The terminal points of the 13-month forecasts are indicated by black dots with crosses. Although the forecasts started from the DA, the first month does not agree exactly, because it is a monthly mean of the forecast.

The SST forecasts, shown in the upper panel, agree quite well with the observations, capturing the temperature increases in 1982/83 and 1986/87 and also the temperature decreases in 1983/84 and 1987/88. During 1984/85 when the anomalies had little change the forecasts again did well. The lower panel is the *ESI* and it should be noted how well it correlates with the NINO-3 SST anomaly. The forecasted *ESI* seems to capture the anomalous behaviour of the heat content associated with the rise and fall of the thermocline and hence yields a good SST prediction.

An additional measure is "the zonal mean of thermocline anomalies" (Li, personal communication), as opposed to the gradient of the thermocline anomalies, i.e. *ESI*. The second measure is of the zonal mean of the 20°C isotherm along the equatorial Pacific, which is defined by

$$MEAN = (D_w + D_E)/210 \tag{3}$$

where $210 = 160 + 50$ see (1). In order to eliminate the seasonality, the anomaly of *MEAN* is calculated. This anomaly is referred to here as the *memory index*.

$$memory\ index = MEAN - \overline{MEAN} \tag{4}$$

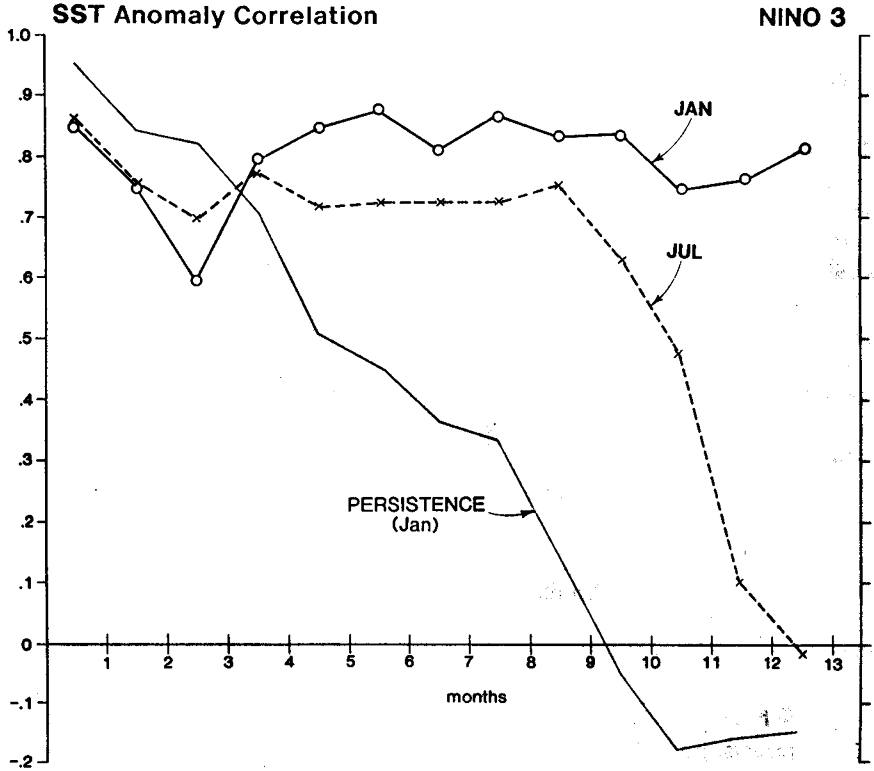

Fig. 2 NINO-3 SST anomaly correlations over the 13-month forecast period. Persistence is also shown for comparison (after Rosati et al., 1997).

According to Schneider et al. (1995), the variables, i.e. the zonal mean heat content anomalies, (4), are not in equilibrium with the wind stress anomalies, implying that they indicate the time tendency of heat content, whereas the heat content anomalies with the zonal mean removed, i.e. *ESI*, are approximately in equilibrium with the wind stress anomalies. This measure will be used later for showing the predictive skill of forecasts.

Figure 2 is a summary of the upper panel in Fig. 1, presenting the NINO-3 skill score curves against prediction time for 7 January and 7 July cases. This diagram confirms the already mentioned facts about the longevity of ENSO forecasts; the scores are significantly above the persistence except for the first 3 months. On the other hand, the far-field forecast scores, i.e. outside of the equatorial zone (not shown here), are limited up to six months, and besides the skill is very low; the scores are below the persistence.

The July score in Fig. 2 is almost comparable to the January score up to the 9th month, and thereafter, it decays rapidly, whereas the persistence curves are almost the same for both the January and July cases. It may be worth noting that the scores are worse than persistence in the first 3 months, and that this feature is very similar both in the January and July cases.

3 Issues on forecast skill

There are a number of issues related to the ENSO forecasts. The subjects we are interested in here are: Forecast error growth, Spring barrier, and Initial dip of forecast skill.

a *Forecast error growth*

According to some model-twin experiments (Gent and Tribbia, 1993), if initial perturbations are given to the vertical temperature distribution of the ocean, the SST error increases rapidly, for example, from 10^{-4}°C to 10^{-1}°C in about two weeks, and as a result, the correlation coefficients (15°N–15°S Pacific basin) drop to 0.5 after 4.5 months. This degree of error growth is normally inevitable, and is known as *predictability decay*. On the other hand, the correlation curves in Fig. 2 decay more slowly than those of Gent and Tribbia. The reason for the high correlation in Fig. 2 may be the fact that El Niño and La Niña forecasts are included, and that the successful forecasts of these extreme events have contributed to raising the forecast skill curves higher than that of Gent and Tribbia.

b *Spring barrier*

It has been argued, based on the Cane-Zebiak model (Cane and Zebiak, 1985), that there is a "prediction barrier" in the spring season and, as a consequence, that the forecasts starting from January are worse than those from July (see Zebiak and Cane, 1987; Blumenthal, 1991; Latif and Graham, 1991; Goswami and Shukla, 1993), though the view has recently been revised (Dr. Busalacchi, personal communication). Webster and Yang (1992) also show, from the lag-lead correlations of the SOI, that May and April emerge as the discontinuity season. As Balmaseda et al. (1994) mentioned, based on the analysis of their simple model forecasts, the correlation skill shows a pronounced drop during spring, often followed by a recovery, due to its memory of the ocean heat content. In other words, the information from the heat content and SST is not lost simultaneously. Comparing the forecasts between the January and July cases in Fig. 2, it appears that the skill score is higher in the January than in the July cases, and that the July score drops in April. However, the sample number in Fig. 2 is too limited to confirm the barrier issue.

c *Initial dip of forecast skill*

In Fig. 2, an inferior performance is evident in the first 3 months. Two possible causes can be considered. One is the "climate drift", because of the model's bias compared with the truth. Another is the improper adjustment of the initial condition to the model's climatology.

The first issue is outside of the scope of the present paper. Concerning the second issue, it appears that a substantial improvement of the initial data and its initialization is desired, perhaps including the precursor of the westerly bursts appropriately (Luther et al., 1983), and refining the model's interactive clouds properly (Gent and Tribbia, 1993). This inferior performance is a definite drawback in the current scheme of Rosati et al. (1997). Investigation should be made as to what extent the coupled model DA can improve this spin-up behaviour.

4 Data assimilation for the coupled system

In order to improve the spin-up problem, and facilitate the ensemble forecasts, a system of data assimilation is developed for the coupled atmospheric-oceanic model.

a *Schemes of the coupled model DA*

The oceanic DA was described in Section 2. The level II oceanic data are: COADS (Comprehensive Ocean Atmospheric Data Set), MOODS (Master Ocean Observation Data Set), NODC (the National Oceanic Data Center), and TOGA (Tropical Ocean and Global Atmosphere Project), which provide the data of surface ocean temperature and the vertical temperature profiles through the XBT.

The atmospheric DA is also based on a continuous injection method but in a different way (Stern and Ploshay, 1992). Level II meteorological data, such as radiosonde measurements, satellite soundings, aircraft reports, etc., are assimilated into the atmospheric GCM, where these data are injected continuously through the OI scheme into the atmospheric model with the help of linear normal mode initialization (Daley and Puri, 1980). In this process, the observed data are treated by taking only the incremental part beyond the first guess, i.e. forecast, and applying the increments to the linear balance in the multivariate framework. This atmospheric system and the resulting analyses have proven to be of comparable accuracy to those of operational centres in 1985 (Ploshay et al., 1992).

In particular, it is a salient feature of this continuous scheme that the initial condition does not produce any spin-up or spin-down effect. On the other hand, the intermittent scheme produces this transient character through the non-linear normal mode initialization, though there has been an effort to reduce this deficiency by introducing non-adiabatic effects (Wergen, 1987).

Using these continuous DA schemes of atmosphere and ocean, two systems of coupled model DA are developed.

1 THE FIRST COUPLED DA

The assimilation is performed through switching the DA for the ocean and the atmosphere alternately at a 6-hour interval. Namely the atmospheric DA is run for 6 hours by inserting the level II meteorological data. The 6-hour averages of wind stress, heat fluxes, and long and short wave incoming radiation are saved to force the ocean model. The ocean model is then run for 6 hours by inserting the level II oceanographic data, and returns the 6-hour averages of SST to be used during the next 6 hours by the atmospheric model.

This coupled DA method requires a 20% increase in computer memory above coupled forecasts. The technical difficulty was to set up the switching process between the atmosphere and the ocean DA. In any event, this technique has been completed and tested successfully. The computer time for the coupled DA is about three times that for the coupled simulation.

2 THE SECOND COUPLED DA

In order to quickly see the effect of coupled DA, a different method was also tested. Using the same DA systems of the atmosphere and the ocean, described under the first coupled DA, the oceanic and the atmospheric DA were processed separately for 10 days, and this separate process was iterated twice. The computer time is therefore twice that for the coupled simulation.

b *Results of the DAs*

The coupled model DAs were applied to construct the 1982 initial conditions. The DA process for the coupled system was started at 10 days before 0000 GMT 1 January 1982. However, the oceanic DA alone had already been run from 1979.

Figures 3a, 3b and 4 show the comparison of resulting atmospheric analysis between the NMC's DA and the coupled model DAs (the first version). The variables are temperature (Fig. 3a) and the zonal wind at the 1000-hPa level (Fig. 3b). There is a tendency for the zonal wind in the coupled DA to be more intense than those of NMC. Figure 4 shows the vertical sections of ocean temperature along the equator, which delineate the thermocline structure in the Pacific. In January 1982, there is already a tendency for the eastern part of the thermocline to be depressed. The top panel is based on the observed atmospheric forcing of the NMC analysis, which is the original DA (Rosati et al., 1995). The middle panel is the result of the first coupled model DA, and the bottom panel is that of the second coupled DA. The difference between the first and the second method is very subtle. The thermoclines (20°C isotherm, for example) are shallower at around 120°W in the coupled DA than in the original DA (top). Furthermore, the second version (bottom) is even shallower than the first version, implying that the structure is more adjusted to the thermocline climatology of this particular coupled model.

It is customarily considered that one of the best ways to evaluate the DA products is to utilize them for forecasts. Using these analyses, 13-month forecasts were carried out. Figures 5a and 5b are Hovmöller (longitude-time) diagrams representing the time evolution of the SST (top), and the depth of 20°C isotherms (bottom). Among them, Fig. 5a does not show forecasts, but the oceanic DA (left), and the ocean simulation (right). The SST fields (left top) are based on Reynolds (1988), and the 20°C isotherm depth (left bottom) is based on Rosati et al. (1995). On the other hand, the top and bottom of the right hand side figures show the results of ocean simulation. Both the ocean DA and simulation are performed by forcing the

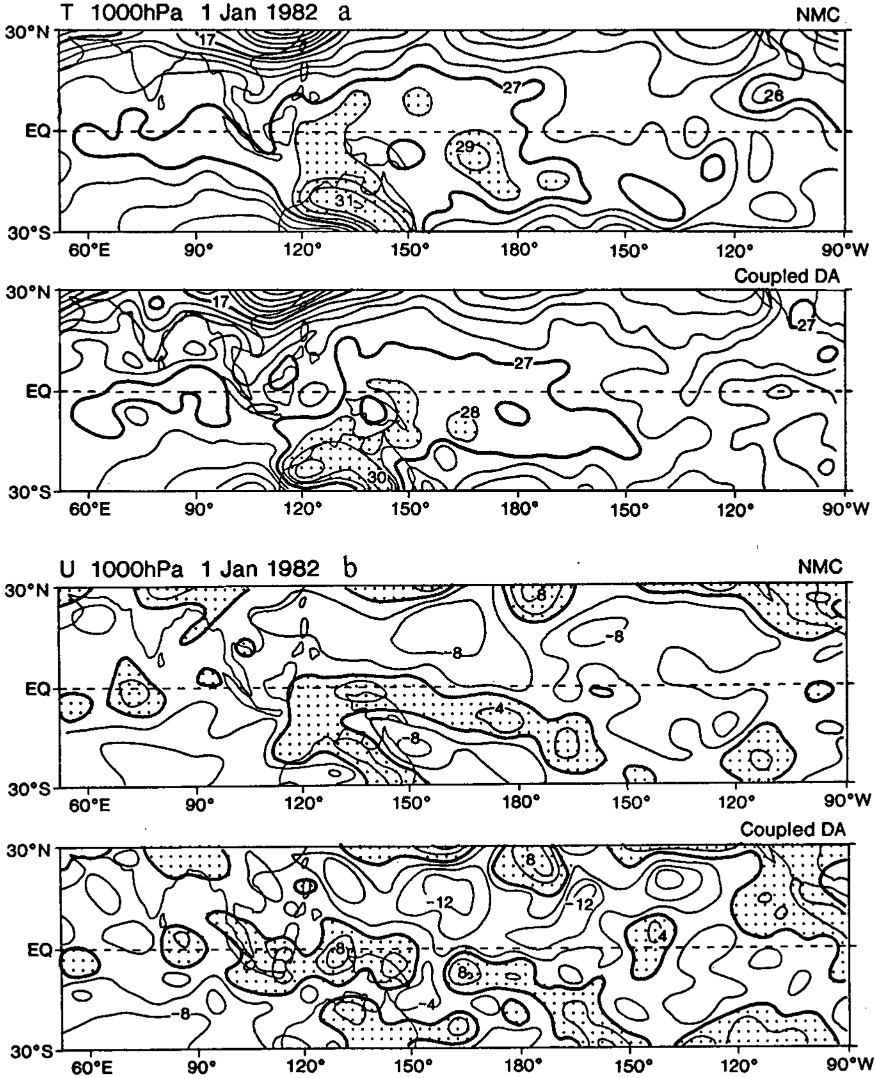

Fig. 3 (a) Comparison of air temperature at 1000-hPa level between the NMC analysis (left) and the coupled DA (right). Units are °C. (b) The same as Fig. 3a but for the zonal wind stress at 1000-hPa level. Units are m s^{-1}.

same observed atmospheric DA at the ocean surface. The only difference between the oceanic DA and the simulation is that the XBT data are used in the former but not in the latter. It may be surprising to note that the patterns of the 20°C isotherm are quite different from each other; it is simply the consequence of the XBT data injection in the former but not in the latter.

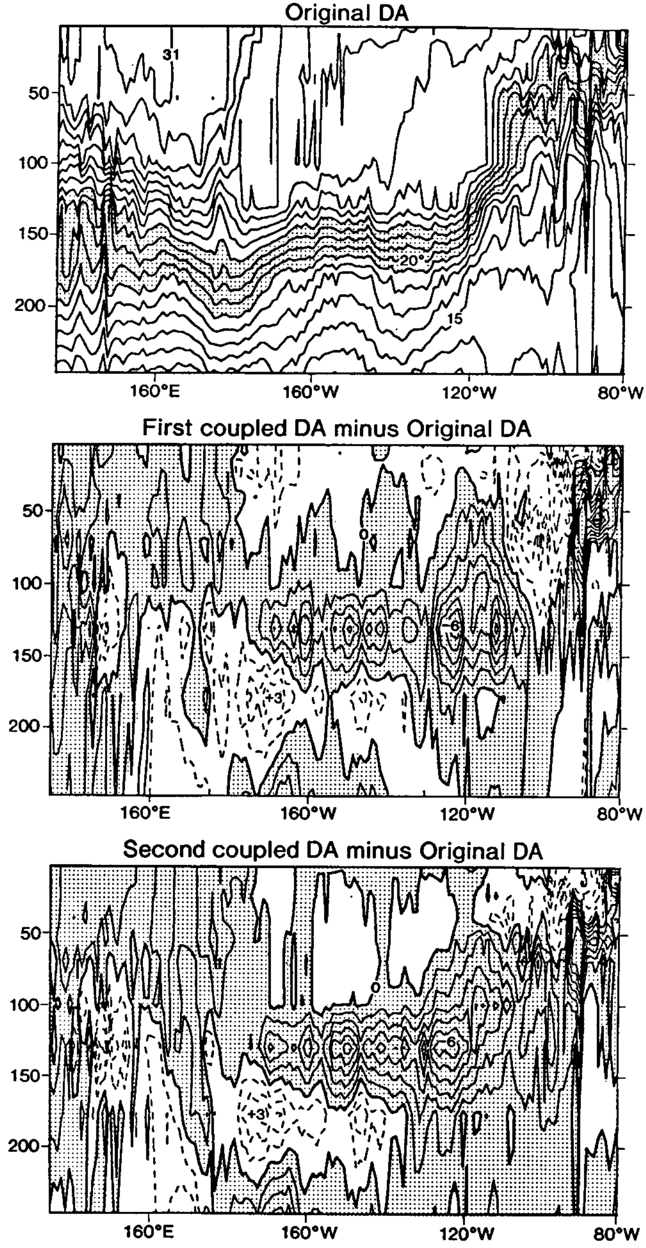

Fig. 4 Longitude-depth section of ocean temperature for January 1982. The oceanic DA (top), the difference of the first coupled DA from the top (middle), and the same for the second coupled DA (bottom). Contour interval is 1°C. Stippling is 19°–23°C (top), and negative values (middle and bottom).

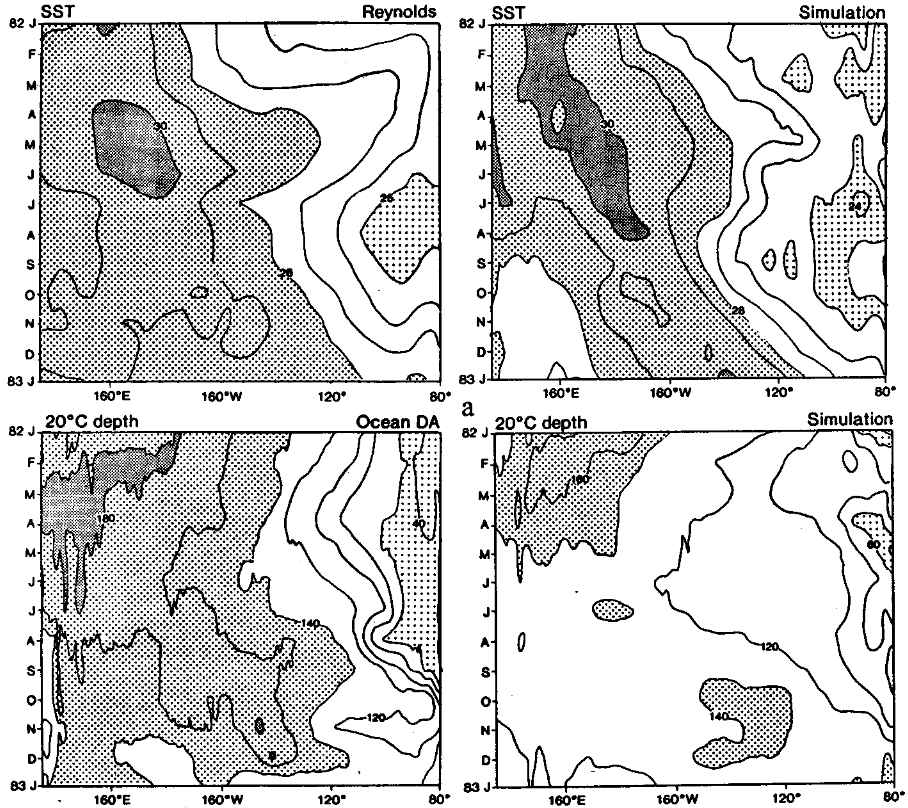

Fig. 5 (a) Longitude-time (Hovmöller) diagrams of SST (top) and 20°C isotherm depth (bottom). The SST of Reynolds analysis (left top), the 20°C depth based on the oceanic DA (left bottom), the SST in simulation (top right), and the 20°C depth (bottom right). Contour intervals are 1°C for SST and 10 m for 20°C depth. (b) The same as Fig. 5a, but all are the results of forecasts. The original (left) is the forecast from the initial conditions of oceanic DA and NMC atmospheric DA; and the forecasts (middle) and (right) are based on the first coupled DA and the second coupled DA.

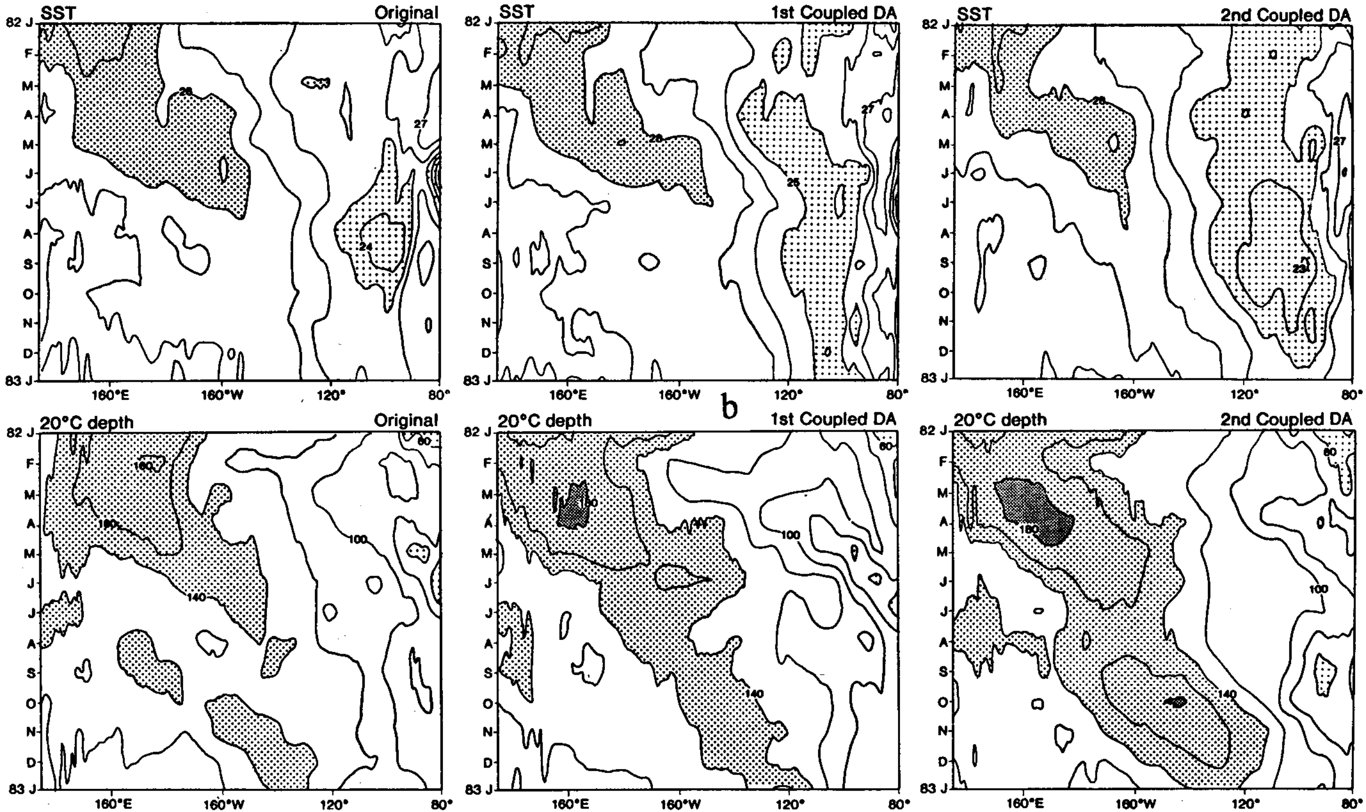

Fig. 5 *(concluded)*.

Figure 5b shows the three forecasts. These results are compared with those of Fig. 5a. The forecast at the left is the same as that of Rosati et al. (1996), which is based on the NMC and the oceanic DA analyses for the initial condition. The forecasts in the middle and at the right are the results from the two initial conditions, i.e. the first and the second coupled DAs. It is a common characteristic in this particular coupled model that the SST in forecasts are considerably lower than the observation (see Fig. 1). This is due to the weaker atmospheric forcing in forecasts by this model (systematic error). Particularly the second coupled DA (far right) gives a different solution from others (far left and middle). The heat content, represented by the 20°C isotherms, propagates eastward more strongly in the second version than in the first version. The last feature is favourable, but from the standpoint of the SST, the forecast (right) deviates considerably from the observation.

To summarize, (a) with respect to the eastward propagation of warm SST, the best forecast is the original one (left), the second is the one based on the initial condition of the first coupled DA (middle), and the third is the one of the second coupled DA (right); (b) on the other hand, the order is just opposite with respect to the development of 20°C isothermal depth. In other words, the second coupled DA gives more model-adjusted and less data-oriented analysis than the first coupled DA or the original DA. This reasoning is consistent with the thermocline structure in Fig. 4. In this respect, the spin-up aspect is best in the second version; a problem is that the SST deviates most from the observation. The only way to improve the situation from both standpoints is through improved physics and resolution in the coupled model.

5 Ensemble forecasts

Using the analyses based on the first version of the coupled DA, forecasts are performed from the initial conditions of 0 day, −2 day, −4 day, and +2 day, for the subsequent 13 months. This decision is not because this version gives the superior forecast, but because we feel that a coupled DA system is the desirable method of the future at GFDL.

a *The case of 1982/83*

Figure 6 displays five curves of SST anomalies in the NINO-3 region; Fig. 7 displays four curves of the ENSO index, *ESI*; and Fig. 8 shows four curves of the memory index. The model's climatology is borrowed from that of Rosati et al. (1996). The five curves (Fig. 6) start to spread in April, and stay separated from each other, the spread being almost the same until January 1983. The ensemble of SST anomalies is considerably lower in amplitude than the observation, the reason being described earlier. It is noted that the forecasts based on the second version of the coupled DA (not shown here) are substantially and unacceptably lower than the group in this figure. The spread (standard deviation) of the ensemble can be calculated, showing that in April, the spread is slightly greater but not substantially large.

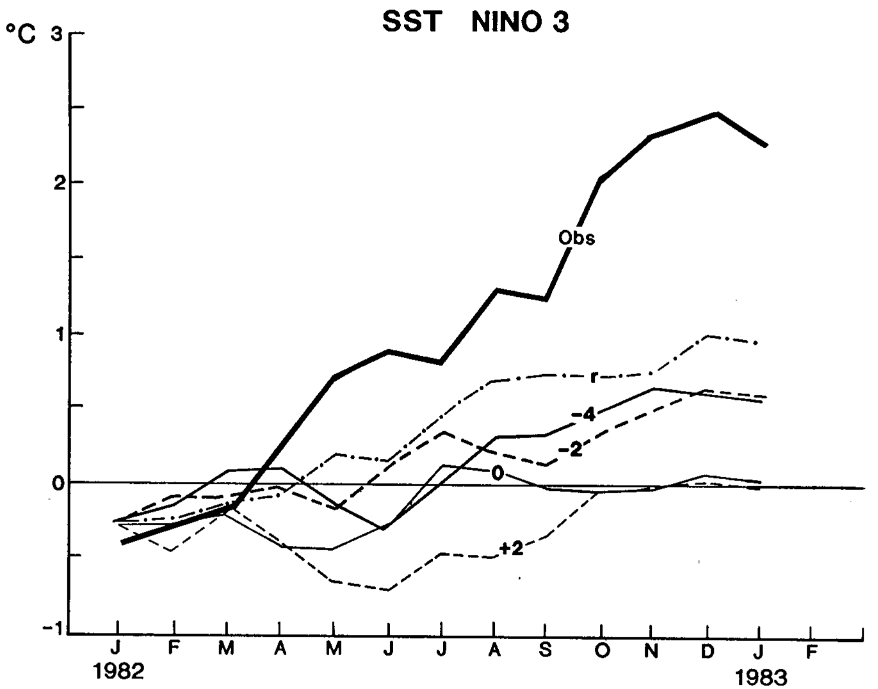

Fig. 6 Performances of 13-month forecasts are shown by SST anomalies for NINO-3 region. The observation (thick curve), and four forecasts from day 0, day −2, day −4, and day +2, based on the initial conditions of the first coupled DA, and a forecast denoted by r, based on the original initial condition, i.e. the oceanic DA and NMC atmospheric DA (Rosati et al., 1997).

Figure 7 shows the ensemble of *ESI*; each member of the four curves behaves similarly; the spread is not large. Here the undulation of three waves may be noticeable; presumably this is arbitrarily caused by a different model climatology that has been borrowed from other forecasts. In any event, it is clear that the *ESI* of these predictions is not sufficiently low, compared with the DA (see Fig. 1). Figure 8 includes the ensemble of the memory index.

b *Preliminary results*

Based on the four member forecasts, two issues are overviewed as a preliminary investigation. Concerning the spread of multiple solutions, there is no serious divergence, meaning that the spring barrier is not recognized, though this is a single case. It is also difficult to conclude that there is an improvement in the spin-up problem. Multiple cases are needed.

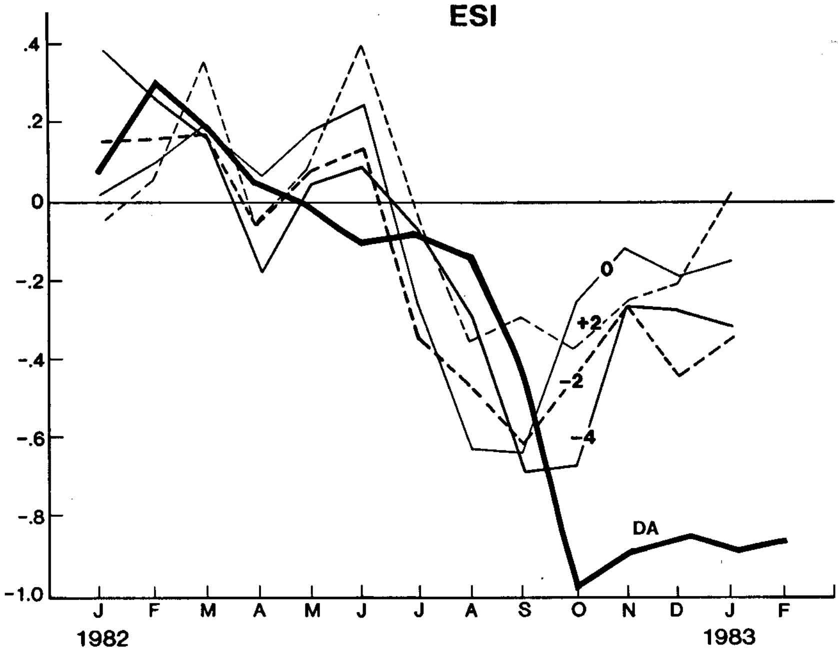

Fig. 7 The same as Fig. 6, but for *ESI*.

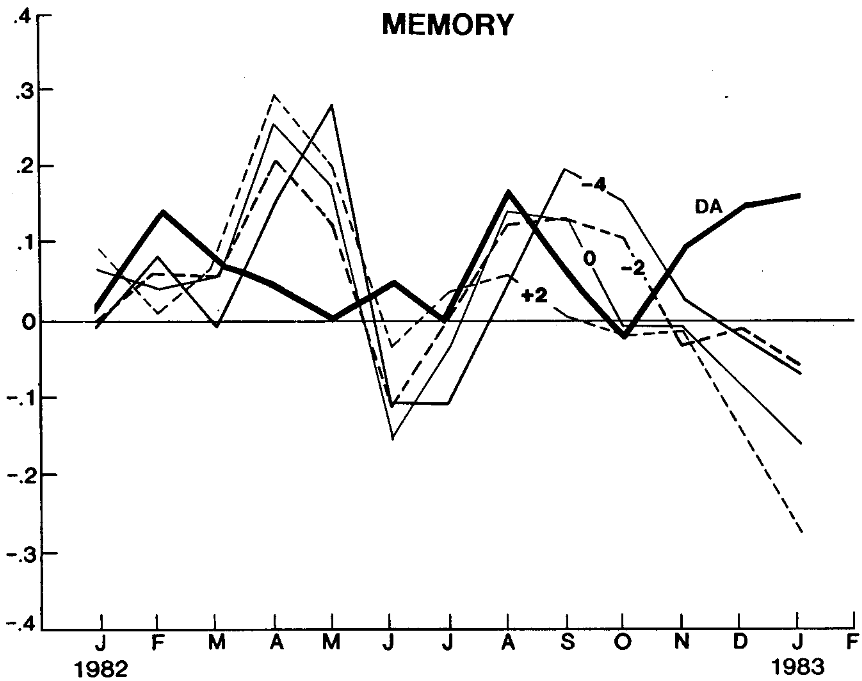

Fig. 8 The same as Fig. 6, but for the memory index.

6 Conclusions and comments

In order to investigate and improve the SST forecast skill associated with El Niño/La Niña events, a coupled atmospheric-oceanic model DA has been developed. The scheme is of the continuous data injection type, in which the GCMs are used for the first guess and the incremental components of observed data beyond the first guess are inserted into the models through the OI. In the atmospheric DA, the dynamic balancing is forced continuously for the incremental parts, while in the oceanic DA, any balancing is not forced (though desirable). These atmospheric and oceanic DAs are applied to the observed data alternately every 6 hours for 10 days, and the initial conditions for the coupled system are obtained (the first coupled DA).

This set of initial conditions is used for the ensemble forecasts as a sample case during the 1982/83 El Niño period. There are two objectives. One is to improve the forecast in the first 3 months, and the other is to investigate whether the "spring barrier" for the equatorial forecasts really exists.

It is tentatively concluded, based on the 4 member forecasts, that the spread of ensemble forecasts for SST is not small for the 13-month forecast range; the spread becomes noticeable after 6 months; however, the spread for the *ESI* or the memory index is not large; the spring barrier is not recognized clearly in this study (see the comment below); and, the spin-up issue is not conclusive due to the limited number of cases. In particular, it is necessary to establish the climatology for this prediction system. In order to discuss the spin-up issue, more forecast cases are needed.

With respect to the spring barrier, an hypothesis is postulated. As is known, the Southern Oscillation has biennial character (see for example, Barnett, 1991), and the separation between the warm and the cold phases is considered. If a 13-month forecast range is within the same phase, the "spring barrier" is not a problem, such as January 1982–January 1983. On the other hand, if the 13-month range crosses from one phase to the other, for example, from January 1983–January 1984, the "spring barrier" may have a disturbing effect. This is an assumption. It will be interesting to apply the ensemble forecasts to other cases.

As has been mentioned with respect to the first coupled DA, the current drawback is due to the large systematic bias of the particular coupled GCM; the SST is substantially lower than the observation, and the surface wind is biased in a certain way. In other words, this GCM is not of a great help for DA. The DA scheme should be modified with respect to the model bias utilizing climatological information.

Acknowledgment

The authors wish to thank William Stern and Richard Gudgel for useful advice. Significant suggestions for improved presentation of the results were offered by Tim Li, and useful advice was provided by Yoshio Kurihara and Jerry Mahlman. Special thanks go to Cathy Raphael, Jeff Varanyak and Wendy Marshall who produced the illustration figures and the manuscript.

References

BALMASEDA, M.A.; M.K. DAVEY and D.L.T. ANDERSON. 1994. Seasonal dependence of ENSO prediction skill. Climate Research Tech. Note, No. 51, Hadley Centre, England, 21 pp.

BARNETT, T.P. 1991. The interaction of multiple time scales in the tropical climate system. *J. Clim.* **4**: 269–285.

———; N. GRAHAM, M. CANE, S. ZEBIAK, S. DOLAN, J. O'BRIEN and D. LEGLER. 1988. On prediction of the El Niño of 1986–87. *Science*, **241**: 109–196.

BLUMENTHAL, M.B. 1991. Predictability of a coupled ocean-atmosphere model. *J. Clim.* **4**: 766–784.

BRANKOVIC, C.; T.N. PALMER and L. FERRANTI. 1994. Predictability of seasonal atmospheric variations. *J. Clim.* **7**: 217–237.

CANE, M.A. and S.E. ZEBIAK. 1985. A theory for El Niño and the Southern Oscillation. *Science*, **228**: 1084–1087.

———; ——— and S.C. DOLAN. 1986. Experimental forecasts of El Niño. *Science*, **321**: 827–832.

DALEY, R. and K. PURI. 1980. Four-dimensional data assimilation and the slow manifold. *Mon. Weather Rev.* **108**: 85–99.

DERBER, J. and A. ROSATI. 1989. A global oceanic data assimilation system. *J. Phys. Oceanogr.* **19**: 1333–1347.

GENT, P.R. and J.J. TRIBBIA. 1993. Simulation and predictability in a coupled TOGA model. *J. Clim.* **6**: 1843–1858.

GOSWAMI, B.N. and J. SHUKLA. 1993. Predictability of a coupled ocean-atmospheric flow. *J. Atmos. Sci.* **4**: 3–22.

LAPRISE, R. 1993. The resolution of global spectral models. *Bull. Am. Meteorol. Soc.* **73**: 1453–1454.

LATIF, M. and N.E. GRAHAM. 1991. How much predictive skill is contained in the thermal structure of an OGCM? *TOGA Notes*, **2**: 6–8.

LUTHER, D.S.; D.E. HARRISON and R.A. KNOX. 1983. Zonal winds in the central equatorial Pacific and El Niño. *Science*, **222**: 327–330.

MIYAKODA, K.; A. ROSATI and R. GUDGEL. 1993. Toward the GCM El Niño simulation. In: *Prediction of Interannual Climate Variations*, J. Shukla (Ed.), NATO ASI Series, 16, Springer-Verlag, Berlin and Heidelberg, pp. 125–151.

NEELIN, J.D.; M. LATIF, M.A.F. ALLAART, M.A. CANE, U. CUBASCH, W.L. GATES, P.R. GENT, M. GHIL, C. GORDON, N.C. LAU, C.R. MECHOSO, G.A. MEEHL, J.M. OBERTUBER, S.G.H. PHILANDER, P.S. SCHOPF, K.R. SPERBER, A. STERL, T. TOKIOKA, J. TRIBBIA and S.E. ZEBIAK. 1992. Tropical air-sea interaction in general circulation models. *Clim. Dyn.* **7**: 75–104.

PHILANDER, S.G.H. and A.D. SEIGEL. 1985. Simulation of El Niño of 1982-83. In: *Coupled Ocean-Atmosphere Models*, J.G.J. Nihoul (Ed.), Elsevier Oceanography Series, No. 40, pp. 517–541.

PLOSHAY, J.J.; W.F. STERN and K. MIYAKODA. 1992. FGGE reanalysis at GFDL. *Mon. Weather Rev.* **120**: 2083–2108.

REYNOLDS, R.W. 1988. A real time global sea surface temperature analysis. *J. Clim.* **1**: 75–86.

ROSATI, A.; R.G. GUDGEL and K. MIYAKODA. 1995. Decadal analysis produced from an ocean data assimilation system. *Mon. Weather Rev.* **123**: 2206–2228.

———; K. MIYAKODA and R.G. GUDGEL. 1997. The impact of oceanic initial conditions on ENSO forecasting with a coupled model. *Mon. Weather Rev.* **125**: 255–273.

SAUSEN, R.; K. BARTHELS and K. HASSELMANN. 1988. Coupled ocean-atmospheric models with flux correction. *Clim. Dyn.* **2**: 154–163.

SCHNEIDER, E.K.; B. HUANG and J. SHUKLA. 1995. Ocean wave dynamics and El Niño. *J. Clim.* **8**: 2415–2439.

STERN, W.F. and J.J. PLOSHAY. 1992. A scheme for continuous data assimilation. *Mon. Weather Rev.* **120**: 1417–1432.

TROUP, A.J. 1965. The Southern oscillation. *Q. J. R. Meteorol. Soc.* **91**: 490–506.

TRENBERTH, K.E. 1976. Spatial and temporal variations of the Southern Oscillation. *Q. J. R. Meteorol. Soc.* **102**: 639–653.

WEBSTER, P.J. and S. YANG. 1992. Monsoon and ENSO. Selectively interactive systems. *Q. J. R. Meteorol. Soc.* **118**: 877–926.

WERGEN, W. 1987. Diabatic non-linear normal mode initialization for a spectral model with a hybrid vertical coordinate. ECMWF Tech. Rept., 59; available from ECMWF, Reading, UK, 83 pp.

ZEBIAK, S.E. and M.A. CANE. 1987. A model El Niño-Southern Oscillation. *Mon. Weather Rev.* **115**: 2262–2278.